JAM CM Journal of Applied Mathematics and Computational Mechanics 2025, 24(1), 5-17
www.amcm.pcz.pl p-ISSN 2299-9965
DOI: 10.17512/jamcm.2025.1.01 e-ISSN 2353-0588

POLLUTION DYNAMICS IN AN INTERCONNECTED LAKE SYSTEM: MODELING AND SIMULATION USING THE FINITE ELEMENT METHOD

***Mohamed Adel*[1], *Mohamed M. Khader*[2,3]**

[1] *Department of Mathematics, Faculty of Science, Islamic University of Madinah, Medina, KSA*
[2] *Department of Mathematics and Statistics, College of Science, Imam Mohammad Ibn Saud Islamic University (IMSIU), Riyadh, KSA*
[3] *Department of Mathematics, Faculty of Science, Benha University, Benha, Egypt*
adel@sci.cu.edu.eg, mmkhader@imamu.edu.sa

Received: 11 July 2024; Accepted: 9 January 2025

Abstract. In this research, we present a real-world simulation to evaluate the pollution dynamics within a network of three interconnected lakes, facilitated by canals. Using the finite element method (FEM), we handle three input models: linear, periodic, and exponentially decaying. This procedure turns the specified model into an algebraic equations system. By analyzing the residual error function (REF), we can verify the offered technique's accuracy and efficiency. The numerical outputs are contrasted with that of the fourth-order Runge-Kutta (RK4M). Our results confirm that the presented algorithm is a practical tool to simulate the solution of such models. Key advantages of the supposed approach include simplicity, absence of secular components, and independence from perturbation parameters.

MSC 2010: *41A10, 65N12, 65N35*
Keywords: *pollution model for the lakes system, finite element method, RK4M, REF*

1. Introduction

The goal of this work is to characterize the pollution of the three-lakes system depicted in Figure 1 [1]. Every lake is regarded as a sizable section, and the canals that connect them are seen as pipes with distinct flow directions. The first lake receives an initial addition of pollutants at a fixed rate that may vary over time. For this reason, we are curious about each lake's current pollution status. It is assumed that the water level in each lake is fixed, and we presume that some mixing procedure evenly distributes the pollutants in each lake. Additionally, we take it for granted that pollution never changes and never takes on new forms. This pollution model for a network of three lakes joined by waterways can be modeled mathematically. This significant model has been examined in numerous research studies [2].

For the pollution source, we will consider the periodic, exponentially decaying, and linear input models. As far as the authors are aware, the fact that published works

have referenced the periodic and exponential decaying input models as potential behaviors for the source of pollution is very limited. Here are many research papers that have examined the pollution model for lakes in its classical and fractional formulation [3–6].

In this field, numerous academics have effectively employed a variety of numerical techniques after these earlier studies [7, 8]. A MATLAB solver, called the fourth--order boundary value problem (bvp4c), was used to solve systems of ordinary differential equations resulting from three problems in fluid mechanics, respectively, time--dependent Blasius-Rayleigh-Stokes flow conveying hybrid nanofluid and heat transfer induced by non-Fourier heat flux and transitive magnetic field [9]; buoyancy effect on the stagnation point flow of a hybrid nanofluid toward a vertical plate in a saturated porous medium [10]; stagnation point flow of a water-based graphene-oxide over a stretching/shrinking sheet under an induced magnetic field with a homogeneous--heterogeneous chemical reactions [11]. Additionally, the FEM is one of these techniques [12, 13]. When dealing with this group of equations, the FEM has some advantages because any numerical programming may simply produce the coefficients for the solution. Because of this, the FEM operates much more quickly than the other methods. Also, one of the great benefits of the FEM is that it allows for the safe simulation of conditions that would be dangerous or difficult to replicate in a physical test environment. The results produced by software using this method are extremely detailed and accurate, and provide a wide range of conditions to test against. Kochnev used the FEM to study the atom [14]. The condensed generalized finite element approach has been thoroughly examined by Zhang & Cui [15]. The resilient and trustworthy FEMs used in poromechanics have been explored by Bertrand et al. [16].

In this paper, we developed the FEM for solving the proposed model, and some stability concepts & existence and uniqueness are also considered.

2. Pollution model formulation

A set of lakes connected by waterways are modeled as large portions connected by pipes [17]. A system with three lakes is shown in Figure 1. For instance, at $t = 0$, a factory $b(t)$ delivers a pollutant at a rate of b into one lake. As seen in [18], the contaminated water then finds its way to the other lakes via pipelines. Assume that all of the lakes have the same amount of pollution and that each lake's water level stays constant. Predicting each lake's pollution rate while accounting for these assumptions for $t \geq 0$ is our goal. To comprehend the dynamic behavior of the lakes, we will utilize the variables V_k and $\psi_k(t)$, for $k = 1, 2, 3$, to represent the water volume and pollutant count in lake k, respectively. The following represents the lake k's pollution concentration at $t \geq 0$:

$$c_k(t) = \frac{\psi_k(t)}{V_k}. \tag{1}$$

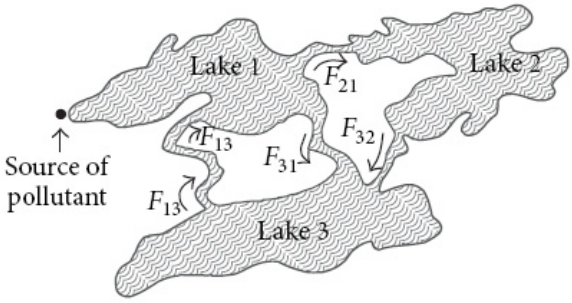

Fig. 1. System of three lakes with waterways connecting them [17]

The flux of pollution $r_{ik}(t)$ evaporating flowing from Lake k into Lake i within the time t is described by the following equation (this outcome occurs by assuming further that there is a constant flow rate F_{ik} between lakes k and i):

$$r_{ik}(t) = F_{ik}\, c_k(t) = \frac{F_{ik}\,\psi_k(t)}{V_k}. \tag{2}$$

By giving each lake the following application of the principle:

The difference between the rates of input and output equals the pollutant change rate, we obtain:

$$\begin{aligned}
\frac{d\psi_1}{dt} &= \frac{F_{13}}{V_3}\psi_3(t) - \frac{F_{31}}{V_1}\psi_1(t) - \frac{F_{21}}{V_1}\psi_1(t) + b(t),\\
\frac{d\psi_2}{dt} &= \frac{F_{21}}{V_1}\psi_1(t) - \frac{F_{32}}{V_2}\psi_2(t),\\
\frac{d\psi_3}{dt} &= \frac{F_{31}}{V_1}\psi_1(t) + \frac{F_{32}}{V_2}\psi_2(t) - \frac{F_{13}}{V_3}\psi_3(t).
\end{aligned} \tag{3}$$

Assuming that the lakes are originally devoid of pollution, the model (3) has the following initial conditions:

$$\psi_1(0) = \psi_2(0) = \psi_3(0) = 0. \tag{4}$$

Every lake's rate of incoming flow equals its rate of departing flow because the volume of water in each lake stays the same for time $t \geq 0$. The following flow rate situations consequently emerge:

$$\begin{aligned}
&\text{Lake } 1 : F_{13} = F_{21} + F_{31},\\
&\text{Lake } 2 : F_{21} = F_{32},\\
&\text{Lake } 3 : F_{31} + F_{32} = F_{13}.
\end{aligned} \tag{5}$$

Remark: From summing the three equations in the model (3), we can obtain the following formula:

$$\frac{d}{dt}[\psi_1(t)+\psi_2(t)+\psi_3(t)] = b(t), \tag{6}$$

this formula and the initial conditions (4) imply that the total pollution in the three lakes can be given by the following form:

$$\psi_1(t)+\psi_2(t)+\psi_3(t) = \int_0^t b(t)dt. \tag{7}$$

This formula will be used later to verify the validity and accuracy of the proposed numerical method in the next sections.

3. Solution process using the FEM

A powerful method for numerically solving ODEs is FEM. This method divides the domain into its constituent Finite Elements. Additionally, this approach is a flexible numerical technique used to research a variety of issues, including fluid mechanics, heat transport, and others.
The stages listed below will be used to implement the FEM, according to [19]:

1. *Finite-element discretization:*
   These elements will be combined to create the finite-element mesh.

2. *Element **equations** derivation:*

   - For every common element removed from the suggested mesh, we offer the variational formulation (VF) of the issue.
   - The element equations are then used to replace the VF's estimated solution.
   - The element interpolation functions are used to construct the stiffness matrix, sometimes referred to as the element matrix.

3. *Collect the element equations:*
   Numerous other algebraic equations can be created by combining the algebraic equations.

4. *Insert the B.Cs:*
   On top of the gathered equations, we apply the fundamental and natural B.Cs.

5. *The ensuing algebraic equations solution:*
   We analyze the set of algebraic equations encountered using any efficient numerical method.

3.1. Variational in formulation

The variational form related to Eqs. (3) is constructed over a typical linear element (t_e, t_{e+1}) as follows:

$$\int_{t_e}^{t_{e+1}} \phi_1 \left[\dot{\psi}_1 - \frac{F_{13}}{V_3}\,\psi_3(t) + \frac{F_{31}}{V_1}\,\psi_1(t) + \frac{F_{21}}{V_1}\,\psi_1(t) - b(t) \right] dt, \tag{8}$$

$$\int_{t_e}^{t_{e+1}} \phi_2 \left[\dot{\psi}_2 - \frac{F_{21}}{V_1}\,\psi_1(t) + \frac{F_{32}}{V_2}\,\psi_2(t) \right] dt, \tag{9}$$

$$\int_{t_e}^{t_{e+1}} \phi_3 \left[\dot{\psi}_3 - \frac{F_{31}}{V_1}\,\psi_1(t) - \frac{F_{32}}{V_2}\,\psi_2(t) + \frac{F_{13}}{V_3}\,\psi_3(t) \right] dt, \tag{10}$$

where the arbitrary test functions $\phi_1,\ \phi_2,\ \phi_3$ can be seen as a change in $\psi_1,\ \psi_2,\ \psi_3$.

3.2. Finite element formulation

We have

$$\psi_1(t) = \sum_{\ell=1}^{2} \psi_{1,\ell}\Upsilon_\ell, \qquad \psi_2(t) = \sum_{\ell=1}^{2} \psi_{2,\ell}\Upsilon_\ell, \qquad \psi_3(t) = \sum_{\ell=1}^{2} \psi_{3,\ell}\Upsilon_\ell, \tag{11}$$

with $\phi_1 = \phi_2 = \phi_3 = \Upsilon_\ell,\ \ell = 1,2$.
The form functions for a typical element (t_e, t_{e+1}) used in our calculations are determined by:
Linear element:

$$\Upsilon_1^e = \frac{t_{e+1} - t}{t_{e+1} - t_e}, \qquad \Upsilon_2^e = \frac{t - t_e}{t_{e+1} - t_e}, \qquad t_e \le t \le t_{e+1}. \tag{12}$$

Quadratic element:

$$\begin{aligned} \Upsilon_1^e &= \frac{(t_{e+1} - t_e - 2t)(t_{e+1} - t)}{(t_{e+1} - t_e)^2}, & \Upsilon_2^e &= \frac{4(t - t_e)(t_{e+1} - t)}{(t_{e+1} - t_e)^2}, \\ \Upsilon_3^e &= -\frac{(t_{e+1} - t_e - 2t)(t - t_e)}{(t_{e+1} - t_e)^2}, & & t_e \le t \le t_{e+1}. \end{aligned} \tag{13}$$

The obtained equations' FEM can be described as follows:

$$\begin{pmatrix} [A^{11}] & [A^{12}] & [A^{13}] \\ [A^{21}] & [A^{22}] & [A^{23}] \\ [A^{31}] & [A^{32}] & [A^{33}] \end{pmatrix} \begin{pmatrix} [\psi_1] \\ [\psi_2] \\ [\psi_3] \end{pmatrix} = \begin{pmatrix} [c^1] \\ [c^2] \\ [c^3] \end{pmatrix}, \tag{14}$$

where $[A^{rs}]$ and $[c^r]$ $(r,s=1,2,3)$ are realized as:

$$A_{ij}^{11}=\int_{t_e}^{t_{e+1}}\left(\Upsilon_i\frac{d\Upsilon_j}{dt}+\frac{F_{21}+F_{31}}{V_1}\left(\Upsilon_i\Upsilon_j\right)\right)dt,\qquad A_{ij}^{12}=0,\qquad A_{ij}^{13}=-\int_{t_e}^{t_{e+1}}\frac{F_{13}}{V_3}\left(\Upsilon_i\Upsilon_j\right)dt,$$
$$A_{ij}^{21}=-\int_{t_e}^{t_{e+1}}\frac{F_{21}}{V_1}\left(\Upsilon_i\Upsilon_j\right)dt,\qquad A_{ij}^{22}=\int_{t_e}^{t_{e+1}}\left(\Upsilon_i\frac{d\Upsilon_j}{dt}+\frac{F_{32}}{V_2}\left(\Upsilon_i\Upsilon_j\right)\right)dt,\qquad A_{ij}^{23}=0,$$
$$A_{ij}^{31}=-\int_{t_e}^{t_{e+1}}\frac{F_{31}}{V_1}\left(\Upsilon_i\Upsilon_j\right)dt,\qquad A_{ij}^{32}=-\int_{t_e}^{t_{e+1}}\frac{F_{32}}{V_2}\left(\Upsilon_i\Upsilon_j\right)dt,$$
$$A_{ij}^{33}=\int_{t_e}^{t_{e+1}}\left(\Upsilon_i\frac{d\Upsilon_j}{dt}+\frac{F_{13}}{V_3}\left(\Upsilon_i\Upsilon_j\right)\right)dt,\qquad c_i^1=\int_{t_e}^{t_{e+1}}\left(\Upsilon_i b(t)\right)dt,\qquad c_i^2=0,\qquad c_i^3=0. \tag{15}$$

4. Some stability concepts & existence and uniqueness

In the past few decades, several stability ideas have been created, such as exponential stability, Lyapunov stability, and others like [20,21]. Next, we verify the stability of the suggested problem using the Banach contraction principle. Let's review some of the key terms from fixed point theory to understand this.

Definition 1. Let $(\Omega,|.|)$ be a metric space. A contraction mapping is defined as follows for any mapping $\mathbb{A}:\Omega\to\Omega$: for every $\varphi_1,\varphi_2\in\Omega$ and $0<\gamma<1$, then:

$$|\mathbb{A}\varphi_1-\mathbb{A}\varphi_2|\leq\gamma|\varphi_1-\varphi_2|. \tag{16}$$

In other words, for every pair of points $\varphi_1,\varphi_2\in\Omega$, is greater than that of points φ_1,φ_2, the ratio,

$$\frac{|\mathbb{A}\varphi_1-\mathbb{A}\varphi_2|}{|\varphi_1-\varphi_2|},$$

doesn't go above the less-than-one positive constant γ.

Let's also review Picard's differential equation existence and uniqueness theorem in the next subsection. Thus, we take into account the first-order IVP that follows:

$$\dot{\Psi}(t)=\mathbb{A}(\Psi,t),\qquad \Psi(t_0)=\Psi_0, \tag{17}$$

with two real numbers, t_0 and Ψ_0, provided.

4.1. Existence and uniqueness

In this subsection, we use the Banach fixed point theorem and the Picard-Lindelöf to show adequate conditions for the existence of a unique solution for the model (17).

Theorem 1. [22]
Let $\mathbb{A}(\Psi,t)$ be continuous on the domain

$$\bar{R} = \{(\Psi,t): \quad |t-t_0| \leq \xi, \quad ||\Psi-\Psi_0|| \leq \sigma\},$$

and thus bounded on $\bar{R}$, i.e. $||\mathbb{A}(\Psi,t)|| \leq \chi$. Suppose that $\mathbb{A}$ satisfies a Lipschitz condition on $\bar{R}$ concerning its first argument, meaning there exists a constant κ such that

$$||\mathbb{A}(\Psi_1,t)-\mathbb{A}(\Psi_2,t)|| \leq \kappa||\Psi_1-\Psi_2||, \qquad \forall\,(\Psi_1,t),(\Psi_2,t) \in \bar{R}.$$

Then the problem (12) has a unique solution that exists on an interval $[t_0-\gamma, t_0+\gamma]$, where

$$\gamma < \min\left\{\xi, \frac{\sigma}{\chi}, \frac{1}{\kappa}\right\}. \tag{18}$$

PROOF You can find the proof in [22]. ∎

5. Numerical simulation

In this part, we address the studied model (3) for three different pollution models and offer a numerical simulation on test examples in $[0,20]$ to test the accuracy of the offered algorithm. However, for the following parameters, we employ the same values throughout all figures:

$$F_{21} = 18\,\text{mi}^3/\text{year}, \quad F_{32} = 18\,\text{mi}^3/\text{year}, \quad F_{31} = 20\,\text{mi}^3/\text{year}, \quad F_{13} = 38\,\text{mi}^3/\text{year},$$
$$V_1 = 2900\,\text{mi}^3, \quad V_2 = 850\,\text{mi}^3, \quad V_3 = 1180\,\text{mi}^3 \tag{19}$$

We will examine the subsequent three input models [23].
Also, we provide a comparison between the results obtained using the recommended approach and the RK4M in each case. In addition, we assess the quality of the presented scheme using the REF [24].
Each case with initial conditions of zeros and the parameter values listed in (19).

Case 1: Periodic input model

When adding pollutants to Lake 1 on a regular basis, this input model is employed. Consider this, for instance:

$$b(t) = \alpha + \beta\sin(\omega t),$$

where ω indicates the frequency of fluctuations, β is the amplitude of fluctuations, and α is the average concentration of pollutants input. Considering $\alpha = \beta = 2$, $\omega = 1$.

The numerical results for the examined example, which were obtained through the use of the suggested methodology, as shown in Figures 2 and 3.

1. In Figure 2, we contrast the results produced using the suggested method and those acquired using the RK4 method in this comparison.
2. In Figure 3, we determine and display the REF of the approximation.

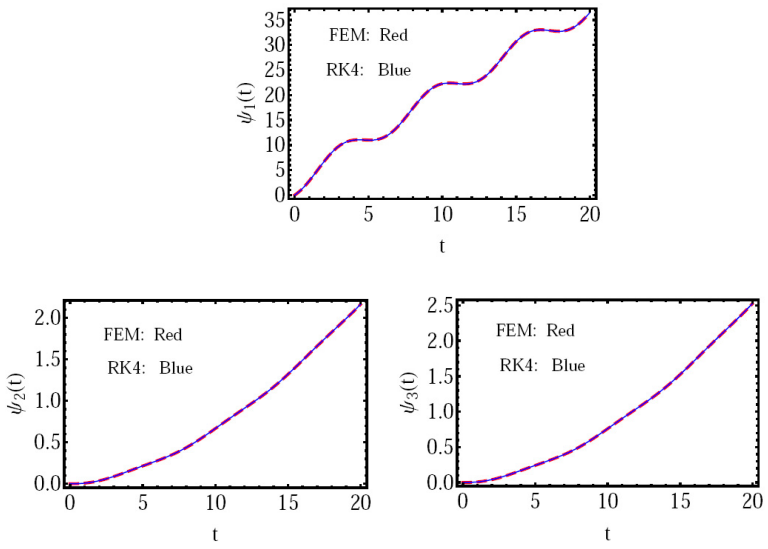

Fig. 2. The solution of case 1, $\psi_i(t)$, $i = 1,2,3$ by the FEM and RK4 methods

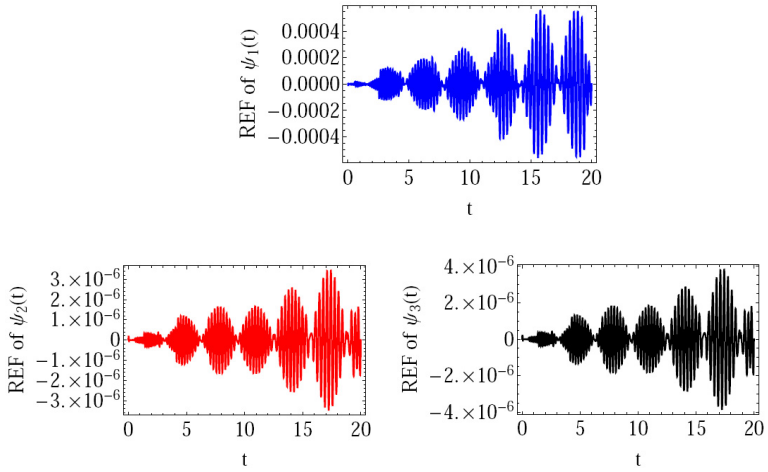

Fig. 3. The REF of $\psi_i(t)$, $i = 1,2,3$ for case 1

Case 2: Exponentially decaying input model

This input model is equivalent to a large-scale pollutant dump. We use the following as an example:

$$b(t) = \mu e^{-\theta t},$$

where $\mu = 150$, $\theta = 15$.

The numerical results for the examined example, which were obtained through the use of the suggested methodology, as shown in Figures 4 and 5.

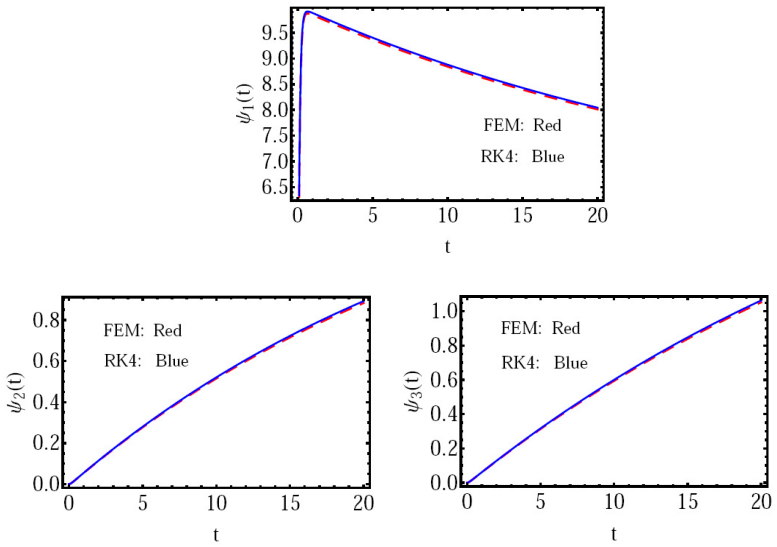

Fig. 4. The solution of case 2, $\psi_i(t)$, $i = 1,2,3$ by the FEM and RK4 methods

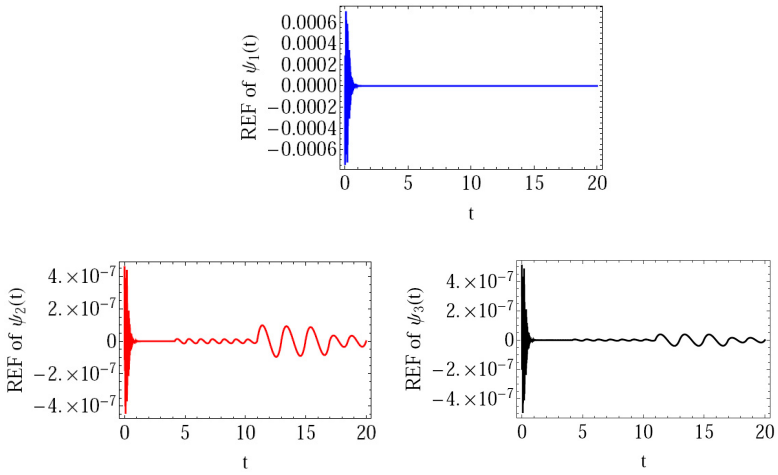

Fig. 5. The REF of $\psi_i(t)$, $i = 1,2,3$ for case 2

1. In Figure 4, we contrast the results produced using the suggested method and those acquired using the RK4 method in this comparison.
2. In Figure 5, we determine and display the REF of the approximation.

Case 3: Linear input model

This input model is used when the pollutant is introduced into the first lake at a linear concentration. As an illustration, consider this:

$$b(t) = \lambda t,$$

where $\lambda = 200$.

The numerical results for this example under investigation were obtained through the use of the suggested methodology, as shown in Figures 6 and 7.

1. In Figure 6, we compare the outcomes obtained using the RK4 approach versus the ones generated by the recommended method.
2. We calculate and plot the estimated solution's REF in Figure 7.

These results show that the efficiency and output of the procedure are greatly enhanced by the suggested methodology.

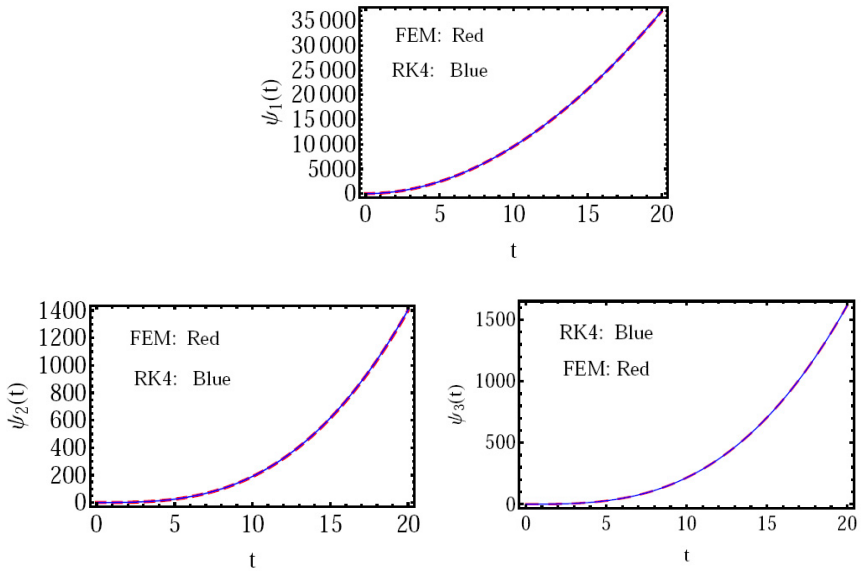

Fig. 6. The solution of case 3, $\psi_i(t)$, $i = 1,2,3$ by the FEM and RK4 methods

In addition, to present more numerical validation of the proposed numerical method, we computed the two sides of the criterion (7) through Tables 1-3 for the three given cases of the model, Periodic, Exponentially, and Linear respectively. The results presented in these three tables confirm that the proposed method is highly effective for the numerical analysis of the model under investigation, yielding significantly improved outcomes.

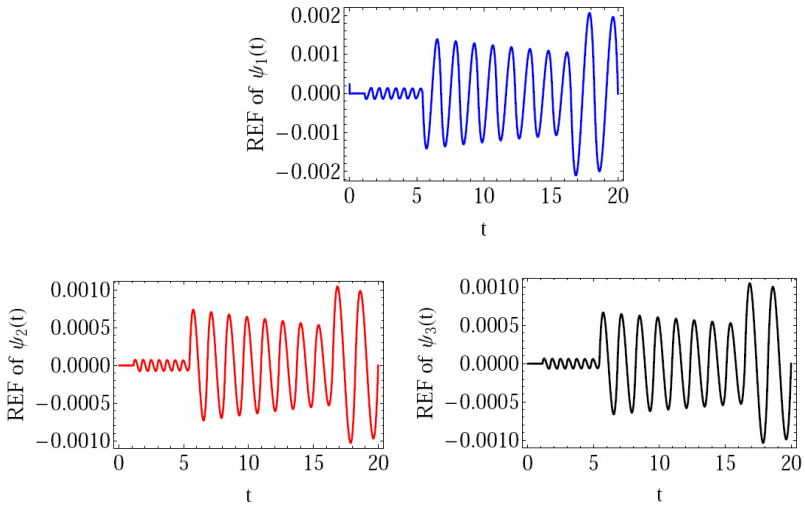

Fig. 7. The REF of $\psi_i(t)$, $i = 1,2,3$ for case 3

Table 1. Comparison of the L.H.S and R.H.S of the criterion (7) for case 1

t	$\psi_1(t)+\psi_2(t)+\psi_3(t)$	$\int_0^t b(t)dt$
0.0	0.000000	0.000000
2.0	6.832290	6.832294
4.0	11.30730	11.30729
6.0	12.07970	12.07966
8.0	18.29100	18.29100
10.0	23.67810	23.67814
12.0	24.31230	24.31229
14.0	29.72650	29.72653
16.0	35.91530	35.91532
18.0	36.67940	36.67937
20.0	41.18380	41.18384

Table 2. Comparison of the L.H.S and R.H.S of the criterion (7) for case 2

t	$\psi_1(t)+\psi_2(t)+\psi_3(t)$	$\int_0^t b(t)dt$
0.0	0.000000	0.000000
2.0	329.6800	329.6800
4.0	550.6710	550.6710
6.0	698.8060	698.8060
8.0	798.1040	798.1040
10.0	864.6650	864.6650
12.0	909.2820	909.2820
14.0	939.1900	939.1900
16.0	959.2380	959.2380
18.0	972.6760	972.6760
20.0	981.6840	981.6840

Table 3. Comparison of the L.H.S and R.H.S of the criterion (7) for case 3

t	$\psi_1(t)+\psi_2(t)+\psi_3(t)$	$\int_0^t b(t)dt$
0.0	0.00	0.00
2.0	400	400
4.0	1600	1600
6.0	3600	3600
8.0	6400	6400
10.0	10000	10000
12.0	14400	14400
14.0	19600	19600
16.0	25600	25600
18.0	32400	32400
20.0	40000	40000

6. Conclusions

The goal of this manuscript is to use the FEM to investigate the dynamic behavior of a lake pollution model. In this attempt, the REF was determined using the numerical solutions of the studied mathematical model. We concluded that the proposed model analysis method works. We can control and reduce error precision by adding terms from the series of approximation solutions. RK4 results are comparable to graphical results. Our results also demonstrate the accuracy and computational efficiency of the proposed method. As an extension of this work, we will address the problem in the future with a more in-depth study, either by presenting a theoretical study to address the stability and convergence of the method used or by trying to provide an improvement in the proposed method.

Acknowledgments

The researchers wish to extend their sincere gratitude to the Deanship of Scientific Research at the Islamic University of Madinah for the support provided to the Post-Publishing Program.

References

[1] Biazar, J., Shahbala, M., & Ebrahimi, H. (2010). VIM for solving the pollution problem of a system of lakes. *Journal of Control Science and Engineering*, *10*, 1-6.

[2] Merdan, M. (2009). Homotopy perturbation method for solving modeling the pollution of a system of lakes. *Fen Dergisi*, *4*(1), 99-111.

[3] Shiri, B., & Baleanu, D. (2022). A general fractional pollution model for lakes. *Communications on Applied Mathematics and Computation*, *4*, 1105-1130.

[4] Kanwal, T., Hussain, A., Avci, I., Etemad, S., Rezapour, S., & Torres D.F.M. (2024). Dynamics of a model of polluted lakes via fractal-fractional operators with two different numerical algorithms. *Chaos, Solitons & Fractals*, *181*, 114653.

[5] Bildik, N., & Deniz, S. (2019). A new fractional analysis on the polluted lakes system. *Chaos, Solitons & Fractals*, *122*, 17-24.

[6] Biazar, J., Farrokhi, L., & Islam, M.R. (2006). Modeling the pollution of a system of lakes. *Applied Mathematics and Computation*, *178*(2), 423-430.

[7] Khader, M.M., & Adel, M. (2020). Numerical approach for solving the Riccati and logistic equations via QLM-rational Legendre collocation method. *Comput. Appl. Math.*, *39*, 1-9.

[8] Adel, M., Sweilam, N.H., & Khader, M.M. (2024). On the stability analysis for a semi-analytical scheme for solving the fractional order blood ethanol concentration system using LVIM. *Journal of Applied Mathematics and Computational Mechanics*, *23*(1), 7-18.

[9] Khan, U., Zaib, A., Ishak, A., & Bakar, S.A. (2021). Time-dependent Blasius-Rayleigh-Stokes flow conveying hybrid nanofluid and heat transfer induced by non-Fourier heat flux and transitive magnetic field. *Case Studies in Thermal Engineering*, *26*, 1-13.

[10] Khan, U., Zaib, A., Bakar, S.A., Roy, N.C., & Ishak, A. (2021). Buoyancy effect on the stagnation point flow of a hybrid nanofluid toward a vertical plate in a saturated porous medium. *Case Studies in Thermal Engineering*, *27*, 1-17.

[11] Khan, U., Zaib, A., Ishak, A., Waini, I., Pop, I., Elattar, S., & Abed, A.M. (2023). Stagnation point flow of a water-based graphene-oxide over a stretching/shrinking sheet under an induced magnetic field with a homogeneous-heterogeneous chemical reaction. *Journal of Magnetism and Magnetic Materials*, *565*, 1-15.

[12] Khader, M.M. (2019). The numerical solution for BVP of the liquid film flow over an unsteady stretching sheet with thermal radiation and magnetic field using the finite element method. *International Journal of Modern Physics C*, *30*(11), 1-8.

[13] Khader, M.M., & Khadijah, M. Abualnaja, (2019). Galerkin-FEM for obtaining the numerical solution of the linear fractional Klein-Gordon equation. *Journal of Applied Analysis and Computation*, *9*(1), 261-270.

[14] Kochnev, V.K. (2021). Finite element method for atoms. *Chemical Physics*, *548*(1), 111197.

[15] Zhang, Q., & Cui, C. (2021). Condensed generalized finite element method. *Numerical Methods in Partial Differential Equations*, *37*, 1847-1868.

[16] Bertrand, F., Ern, A., & Radu, F.A. (2021). Robust and reliable finite element methods in poromechanics. *Computers and Mathematics with Applications*, *91*(1), 1-21.

[17] Yuzbas, S., Sahin, N., & Sezer, M. (2012). A collocation approach to solving the model of pollution for a system of lakes. *Mathematical and Computer Modelling*, *55*(3), 330-341.

[18] John, H. (2006). *Lake Pollution Modelling*. Virginia Tech.

[19] Rana, P., & Bhargava, R. (2012). Flow and heat transfer of a nanofluid over a nonlinear stretching sheet: A numerical study. *Commun. Nonlinear Sci. Numer. Simulat.*, *17*, 212-226.

[20] Dong, Y., Tang, X., & Yuan, Y. (2020). Principled reward shaping for reinforcement learning via Lyapunov stability theory. *Neurocomputing*, *393*, 83-90.

[21] Adel, M., Sweilam, N.H., & Khader, M.M. (2023). Semi-analytical scheme with its stability analysis for solving the fractional-order predator-prey equations by using Laplace-VIM. *Journal of Applied Mathematics and Computational Mechanics*, *22*(4), 5-17.

[22] Adel, M., & Khader, M.M. (2023). Theoretical and numerical treatment for the fractal-fractional model of pollution for a system of lakes using an efficient numerical technique. *Alexandria Engineering Journal*, *82*(1), 415-425.

[23] Benhammouda, B., Leal, H.V., & Martinez, L.H. (2014). Modified DTM for solving the model of pollution for a system of lakes. *Discrete Dynamics in Nature and Society*, *2014*, 1-12.

[24] El-Hawary, H.M., Salim, M.S., & Hussien, H.S. (2003). Ultraspherical integral method for optimal control problems governed by ODEs. *Journal of Global Optimization*, *25*(3), 283-303.